

ChemComm

Accepted Manuscript



This is an *Accepted Manuscript*, which has been through the Royal Society of Chemistry peer review process and has been accepted for publication.

Accepted Manuscripts are published online shortly after acceptance, before technical editing, formatting and proof reading. Using this free service, authors can make their results available to the community, in citable form, before we publish the edited article. We will replace this *Accepted Manuscript* with the edited and formatted *Advance Article* as soon as it is available.

You can find more information about *Accepted Manuscripts* in the [Information for Authors](#).

Please note that technical editing may introduce minor changes to the text and/or graphics, which may alter content. The journal's standard [Terms & Conditions](#) and the [Ethical guidelines](#) still apply. In no event shall the Royal Society of Chemistry be held responsible for any errors or omissions in this *Accepted Manuscript* or any consequences arising from the use of any information it contains.

Iron-Dependent Lysosomal Dysfunction Mediated by a Natural Product Hybrid

Received 00th January 20xx,
Accepted 00th January 20xx

A. Mariani,^a T. T. Mai,^{a,b,c} E. Zacharioudakis,^a A. Hienzsch,^a A. Bartoli,^a T. Cañeque,^{a,b,*} R. Rodriguez^{a,b,c,*}

DOI: 10.1039/x0xx00000x

www.rsc.org/

Artesumycin is a fluorescent hybrid of the natural products marmycin A and artemisinin. It was designed to combine the lysosomotropic property of the angucycline and the iron-reactive capacity of the endoperoxide to target the lysosomal compartment of cancer cells. Herein, we show that artesumycin inhibits cancer cell proliferation in an iron-dependent manner and chemically fragments *in vitro* in the presence of redox-active iron(II). Visual detection of artesumycin by fluorescence microscopy provided substantial evidence that the small molecule selectively targets lysosomes. This original approach based on a fluorescent and iron-reactive probe represents a powerful strategy for initiating and, concomitantly, visualizing lysosomal dysfunction in human cells.

Lysosomes play a crucial role in cellular recycling processes. Biomolecules and organelles targeted for degradation are dismantled in essential building blocks for metabolic reuse.¹ Alteration of the lysosomal membrane integrity, an event known as lysosomal membrane permeabilization (LMP), results in gradual leakage of hydrolytic enzymes into the cytosol, thereby activating cell death signalling pathways.^{1,2} Oxidative stress and lysosomotropic small molecules can promote LMP, representing promising strategies for cancer therapy.^{1,2} The antimalarial and antiproliferative drug artesunate (**1**, Figure 1A), derived from artemisinin, has been reported to functionally damage the endolysosomal compartment through the production of reactive oxygen species (ROS), whose formation is catalysed by the high lysosomal content of redox-active free iron.^{3,4} We have recently described the total synthesis of the angucycline marmycin A (**2**, Figure 1A), and reported the finding that this natural product elicits cell death by accumulating in lysosomes.⁵

We designed the small hybrid molecule artesumycin (**3**, Figure 1A), a dimer of marmycin A and artesunate, with the view to combine the lysosomotropic property of marmycin A with the ROS-generating capacity of artemisinin in a single architecture.⁵ Remarkably, artesumycin displayed a potent growth inhibitory effect against human osteosarcoma U2OS cells compared to marmycin A and artesunate with IC₅₀ values of 0.23, 14 and 1.1 μM, respectively (Figure 1A). This data suggested a mechanistic synergy against the lysosome, which we sought to investigate.

Artesumycin red fluorescence enabled to study the effect of its

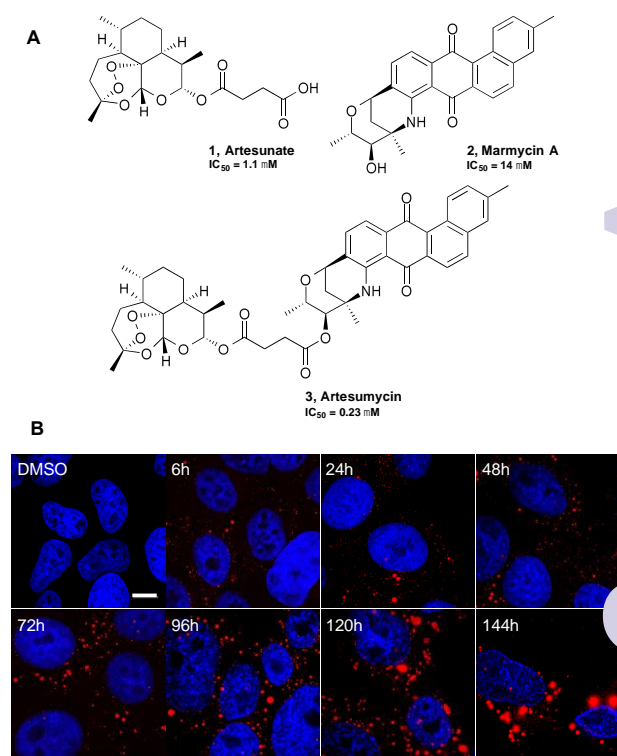


Figure 1. A) Molecular structures of artesunate (**1**), marmycin A (**2**), and artesumycin (**3**) and IC₅₀ values against U2OS cells after 72 h treatment. B) Fluorescence microscopy images of U2OS cells treated with 5 μM of artesumycin (red) for the indicated time. DAPI (blue) stains nuclear DNA. Scale bar: 10 μm.

^a Centre de Recherche de Gif, Institut de Chimie des Substances Naturelles du CNRS, 1 Avenue de la Terrasse, 91198 Gif sur-Yvette, France.

^b Institut Curie Research Center, Organic Synthesis and Cell Biology Group, 26 rue d'Ulm, 75248 Paris Cedex 05, France.

^c CNRS UMR 3666, 75005 Paris, France.

Electronic Supplementary Information (ESI) available: synthetic procedures, bioassays and MS spectra. See DOI: 10.1039/x0xx00000x

prolonged exposure at the single-cell level by means of microscopy. Like marmycin A, we found that artesumycin co-localized with the lysosomal protein GFP-Lamp1 (Figure S1, supporting information). A time-course experiment revealed a progressive increase in size of targeted vesicles consistent with the idea that artesumycin induced a lysosomal dysfunction (Figure 1B).

To investigate the contribution of the lysosomal iron pool to the antiproliferative activity of artesumycin, we measured cell

viability of U2OS cells in the presence of the iron chelator deferoxamine (DFO), known to specifically target lysosomal iron following endocytic uptake.^{4a} Co-treatment with DFO significantly decreased the growth inhibitory property of artesumycin ($IC_{50} = 3.03 \mu\text{M}$). In contrast, co-treatment of these cells with ferric ammonium citrate (FAC) potentiated the cell killing ability of artesumycin ($IC_{50} = 0.12 \mu\text{M}$).⁶ Together, these data implicated lysosomal iron in the cellular activity of artesumycin, encouraging us to investigate the chemical

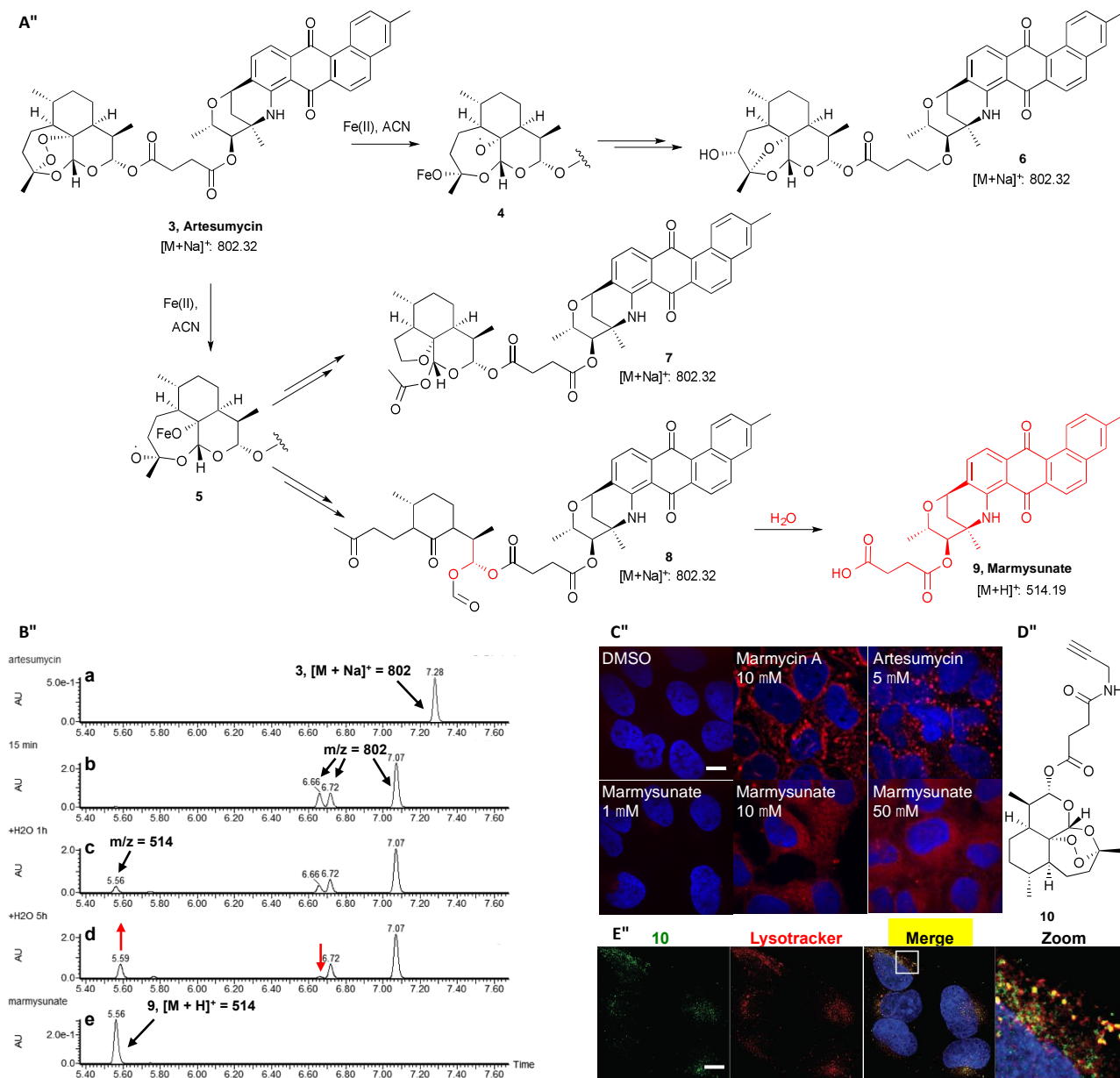


Figure 2. A) Proposed mechanism for the iron-mediated fragmentation of artesumycin. B) UPLC-MS traces of the indicated reactions to monitor the iron-mediated fragmentation of artesumycin: a, artesumycin standard; b, composition of the mixture 15 min after addition of iron(II); c, composition of the mixture 1 h after further addition of water; d, composition of the mixture 5 h after further addition of water; e, synthetic marmysunate standard. C) Fluorescence microscopy images of U2OS cells independently treated with marmycin A (10 μM), artesumycin (5 μM) or marmysunate (1, 10, 50 μM). D) Molecular structure of artesunate-alkyne (10). E) Fluorescence microscopy images of U2OS cells treated with 10 μM of 10, then subjected to click-labeling. Labeled 10 (green) and lysotracker (red). Co-localizing foci can be seen as yellow vesicles in the merge image. The white box indicates the area of magnification of the main image. Zoom image is $\times 5$. Scale bar: 10 μm .

reactivity of the small molecule in the presence of iron *in vitro*. Upon incubation of artesumycin with $\text{FeCl}_2 \cdot 4\text{H}_2\text{O}$ in acetonitrile in a flask, the hybrid molecule was quantitatively converted into three main products as defined by the formation of three ion peaks exhibiting the mass of artesumycin with distinct retention times (802, $[\text{M}+\text{Na}]^+$, Figure 2A, B and Figure S2, supporting information). This data was consistent with a rearrangement of the artesumycin framework mediated by iron. In line with this, no such rearrangement could be observed upon prolonged exposure of artesumycin in acetonitrile in absence of iron. A unified mechanism for the iron-mediated fragmentation of artemisinin-like compounds has previously been proposed, emphasising the central role played by the endoperoxide bridge, implicating Fenton-type chemistry.^{7,8} Thus, we envisioned a fragmentation pathway in which the reductive scission of the peroxide bond could trigger the formation of the two possible O-centered radicals **4** and **5** (Figure 2A). While subsequent rearrangements of **4** was expected to predominantly lead to the formation of product **6**, radical **5** could be engaged in two alternative routes leading either to product **7** or **8**.⁷ Moreover, we anticipated that the labile acetal function of **8** could readily be hydrolysed to yield product **9**. Although the distribution of products was found to be constant overtime in pure acetonitrile (Figure S3, supporting information), addition of water triggered the formation of an additional signal at 5.59 mins exhibiting the mass of **9** ($m/z = 514$, $[\text{M}+\text{H}]^+$, Figure 2A, B and Figure S4, supporting information) at the expense of the signal at 6.66 mins for which the mass was consistent with the proposed structure of intermediate **8**. To confirm this, compound **9**, which we named marmysunate, was independently synthesized in 19 steps taking advantage of our previously reported synthesis of marmycin A.⁵ We found that synthetic marmysunate and product **9** obtained from artesumycin fragmentation exhibited identical masses and retention times (Figure 2A,B and Figure S4, supporting information). The iron-mediated generation of marmysunate represents a unique feature of artesumycin, which helps rationalize the enhanced antiproliferative properties obtained from coupling marmycin A and artesunate in a single scaffold. It is conceivable that in addition to the production of ROS, the release of the carboxylate-containing marmysunate contributed to lysosomal dysfunction once produced in the lysosome. It is noteworthy that synthetic marmysunate exhibited a diffused cytosolic distribution in U2OS cells consistent with the fact that this more water soluble analogue of marmycin A was refractory to direct lysosome targeting, exhibiting instead a higher tropism for the cytosol (Figure 2C). In strong agreement with the notion that artesumycin elicits its activity through lysosomes targeting, synthetic marmysunate was poorly active. To further evaluate the impact of the lipophilic scaffold of the angucycline and its ability to drag the more polar endoperoxide of artesunate into the lysosomal compartment, we synthesized a clickable analogue of artesunate (**10**, Figure 2D). Chemical labeling of small molecules in cells by means of click chemistry enables the visual detection and subcellular

localisation of biologically active compounds.⁹ Interestingly, while we could observe some degree of co-localization of **10** with the lysosomal marker lysotracker, we could also detect green vesicles of the labeled probe **10** that did not co-localize with lysosomes (Figure 2E). Our data suggest that, in addition to its pronounced iron-reactive property to generate ROS, artesumycin exerts its activity partly because of the ability of the angucycline scaffold to facilitate endocytosis or to favour the accumulation of the endoperoxide fragment into lysosomes, which could otherwise remain partly sheltered from iron and thus unable to produce deleterious ROS. Altogether, our data strongly suggest a functional role of the angucycline scaffold, driving the endoperoxide in lysosomes, which upon Fenton-type chemistry leads to the production of ROS and subsequent release of the marmysunate inside this compartement to promote lysosomal dysfunction. This approach, reminiscent of a 'reciprocal prodrug-effect', demonstrates the value of combining complementary physicochemical properties of natural products within a single scaffold to synergistically target an organelle and kill cancer cells.¹⁰ Additional work is required to delineate in full detail the death pathways associated to lysosomal dysfunction linked to treatment with artesumycin. Nevertheless, this molecular probe enables the targeting of lysosomes and visual detection of this targeting. Thus, artesumycin will be instrumental for future studies of lysosome biology as a powerful iron-dependent probe capable of initiating and, concomitantly, visualizing lysosomal dysfunction.

Acknowledgments

We thank the CNRS for funding. Research in R.R.'s laboratory is supported by the European Research Council (grant no. 647973), the Fondation pour la Recherche Médicale (grant no. AJE20141031486), the Emergence Ville de Paris Program and the Ligue Nationale Contre le Cancer. R.R. receives his salary from the CNRS.

Notes and references

- 1 a) P. Kreuzaler and C. J. Watson, *Nat. Rev. Cancer*, 2012, **12**, 411 – 424; b) L. Galluzzi, J. M. Bravo-San Pedro and G. Kroemer, *Nat. Cell. Biol.*, 2014, **16**, 728 – 736.
- 2 L. Groth-Pedersen and M. Jäättelä, *Cancer Lett.*, 2013, **332**, 265 – 274.
- 3 a) D. L. Klayman, *Science*, 1985, **228**, 1049 – 1055; b) J. Wiesner, R. Ortmann, H. Jomaa and M. Schlitzer, *Angew. Chem.* 2003, **115**, 5432 – 5451; *Angew. Chem. Int. Ed.*, 2003, **42**, 5274 – 5293; c) A. Hamacher-Brady, H. A. Stein, S. Turschner, I. Toegel, R. Mora, N. Jennewein, T. Efferth, R. J. and N. R. Brady, *J. Biol. Chem.*, 2011, **286**, 6587 – 6601; d) N.-D. Yang, S.-H. Tan, S. Ng, Y. Shi, J. Zhou, K. S. W. Tan, W.-S. F. Wong and H.-M. Shen, *J. Biol. Chem.* 2014, **289**, 33425 – 33441.
- 4 a) T. Kurz, A. Leake, T. Von Zglinicki and U. T. Brunk, *Biochem. J.*, 2004, **378**, 1039 – 1045; b) G. Kroemer and M. Jäättelä, *Nat. Rev. Cancer*, 2005, **5**, 886 – 897; c) T. Kurz, A. Terman, B. Gustafsson and U. T. Brunk, *Histochem. Cell Biol.*, 2008, **129**, 389 – 406; d) S. J. Dixon and B. R. Stockwell, *Nat. Chem. Biol.* 2014, **10**, 9 – 17.

COMMUNICATION

Journal Name

- 5 T. Cañeque, F. Gomes, T. T. Mai, G. Maestri, M. Malacria and R. Rodriguez, *Nat. Chem.*, 2015, **7**, 744 – 751.
- 6 D. Richardson and E. Baker, *J. Biol. Chem.*, 1992, **267**, 13972 – 13979.
- 7 W.-M. Wu, Y. Wu, Y.-L. Wu, Z.-J. Yao, C.-M. Zhou, Y. Li and F. Shan, *J. Am. Chem. Soc.*, 1998, **120**, 3316 – 3325.
- 8 a) G. H. Posner and C. H. Oh, *J. Am. Chem. Soc.*, 1992, **114**, 8328 – 8329; b) G. H. Posner, D. Wang, J. N. Cumming, C. H. Oh, A. N. French, A. L. Bodley and T. A. Shapiro, *J. Med. Chem.*, 1995, **38**, 2273 – 2275; c) C. W. Jefford, M. G. H. Vicente, Y. Jacquier, F. Favarger, J. Mareda, P. Millasson-Schmidt, G. Brunner and U. Burger, *Helv. Chim. Acta*, 1996, **79**, 1475 – 1487; d) Y. Wu, Z.-Y. Yue and Y.-L. Wu *Angew. Chem.*, 1999, **111**, 2730 – 2733; *Angew. Chem. Int. Ed.*, 1999, **38**, 2580 – 2582; e) A. Robert, J. Cazelles and B. Meunier, *Angew. Chem.*, 2001, **113**, 2008 – 2011; *Angew. Chem. Int. Ed.*, 2001, **40**, 1954 – 1957.
- 9 a) R. Rodriguez, K. M. Miller, J. V. Forment, C. R. Bradshaw, M. Nikan, S. Britton, T. Oelschlaegel, B. Xhemalce, S. Balasubramanian and S. P. Jackson, *Nat. Chem. Biol.*, 2012, **8**, 301 – 310; b) D. Larrieu, S. Britton, M. Demir, R. Rodriguez and S. P. Jackson, *Science*, 2014, **344**, 527 – 532; c) R. Rodriguez and K. M. Miller, *Nat. Rev. Genet.*, 2014, **15**, 783 – 796.
- 10 P. M. O'Neil, P. A. Stocks, M. D. Pugh, N. C. Araujo, E. E. Korshin, J. F. Bickley, S. A. Ward, P. G. Bray, E. Pasini, J. Davies, E. Verissimo and M. D. Bachi, *Angew. Chem.*, 2004, **116**, 4289 – 4293; *Angew. Chem. Int. Ed.*, 2004, **43**, 4193 – 4197.

ChemComm Accepted Manuscript